

Optical design of the NSRL undulator beamline

Y. W. Zhang,* L. S. Sheng, G. B. Zhang and H. Gao

National Synchrotron Radiation Laboratory, University of Science and Technology of China, Hefei, Anhui 230029, People's Republic of China.

E-mail: ywzhang@mail.nslr.ustc.edu.cn

(Received 4 August 1997; accepted 6 January 1998)

The optical design of the NSRL undulator beamline is presented. The NSRL undulator has 29 periods of 9.2 cm that produce a photon energy of 7.7–124 eV with the fundamental and third harmonics at a ring energy of 800 MeV. The beamline consists of a typical Kirkpatrick–Baez prefocusing mirror system, a modified spherical-grating monochromator (SGM) and a refocusing toroidal mirror. The monochromator has two including angles of 148 and 157° with two plane mirrors inserted into the entrance arm in order to cover the wide energy range with high grating diffraction efficiency. Calculation shows that the resolving power of the monochromator can be greater than 5000 with the slits fully opened and 20000 with a 20 µm opening of the slits. The spot at the sample is about 1.5 (H) mm × 0.5 (V) mm.

Keywords: VUV; monochromators; undulators.

1. Introduction

The Hefei Light Source will be equipped with a 2.67 m undulator that produces radiation from 7.7 to 124 eV for atomic and molecular science studies. We need to build a monochromator that has good performance in this energy range and also satisfies the user's requirements. Our task is quite difficult because the monochromator must work in such an energy range that the lower-energy side generally uses a normal-incidence monochromator and the higher-energy side uses a grazing-incidence monochromator.

A toroidal-grating monochromator can be used for this energy range, e.g. the BESSY TGM-1 to -4 and TGM-7, but the resolving power is not high enough for our purpose. In principle, the modified SX-700 (Mythen *et al.*, 1992) or FSGM (Peatman *et al.*, 1995) type monochromators can satisfy our requirements, but the

monochromator mechanism is not easy to construct. The Dragon spherical-grating monochromator (SGM) (Chen, 1987) is one of the most successful monochromators of the past ten years. It has a simple mechanism and can be used for high-resolution experiments. It is widely used in many synchrotron radiation facilities for the energy range from about 10 eV to 1 keV (Chen & Sette, 1989; McKinney *et al.*, 1990; Heimann *et al.*, 1992; Randall *et al.*, 1992; Shu *et al.*, 1989), but none has been used for the range from a few eV to about 100 eV, up to now.

This paper presents a slightly modified SGM design for the NSRL undulator radiation in the energy range from 7.7 to 124 eV. Fig. 1 shows the optical layout. It consists of a typical Kirkpatrick–Baez prefocusing mirror system, a modified spherical-grating monochromator and a refocusing mirror. The expected resolving power is larger than 5000 with the slits fully opened (80 µm) and 20000 with a 20 µm slit opening at 10 eV. The spot at the sample is about 1.5 (H) mm × 0.5 (V) mm.

2. Undulator source

The undulator was designed according to the long-straight-section length of the storage ring and requirements of the atomic and molecular science users. It is 2.67 m long and has 29 periods. The electron energy of the storage ring is 800 MeV and the designed maximum horizontal deflection, K , of the undulator is 3.88, so the first- and third-harmonic energy ranges are 7.7–56 eV and 25–124 eV, respectively. The source size is 0.16 mm (Σ_y) × 1.7 mm (Σ_x). The angular source divergences Σ'_y and Σ'_x depend very much on the energy: they decrease rapidly from 0.25 mrad at 7.7 eV to 0.14 mrad at 30 eV, and then approach slowly about 0.1 mrad at 124 eV. The maximum radiation power is 67 W at 300 mA ring current and 800 MeV electron energy.

There are two water-cooled OFHC copper blocks installed in the photon beam at 5460 mm and 7100 mm, respectively, downstream of the middle of the undulator, which can be moved both horizontally and vertically outside the vacuum. The first has a pinhole of 0.5 mm diameter and is followed by a photon diode, which is used for determining the axis of the undulator beam. The second has one pinhole and three apertures. The pinhole is also 0.5 mm in diameter and followed by a photon diode, which has the same function as the first. The three apertures are determined by the effective undulator source size and divergence at energies of 8, 15 and 30 eV. They are used to prevent unwanted radiation from entering the beamline.

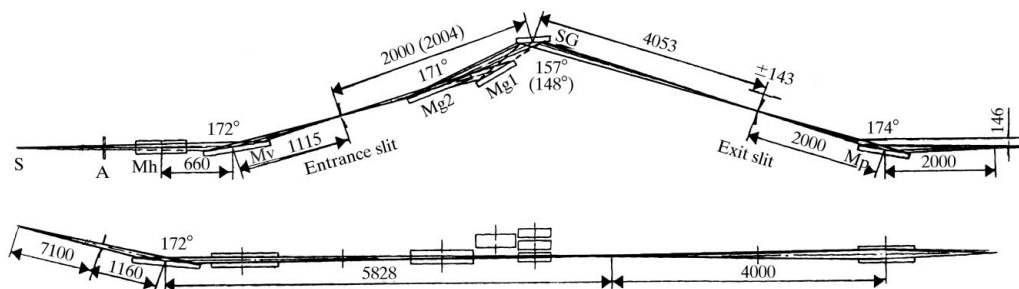


Figure 1
Layout of the NSRL undulator beamline.

Table 1
Basic parameters of the modified spherical-grating monochromator.

	First grating	Second grating	Third grating
Groove density (lines mm ⁻¹)	450	900	1240
Grating profile	Laminar, 1:0.65	Laminar, 1:0.6	Laminar, 1:0.65
Energy range (eV)	7.7–22.5	15–45	36–124
Including angle	148°	148°	157°
Entrance arm length, r_1 (mm)	2004	2004	2000
Exit arm length, r_2 (mm)	4053 ± 143	4053 ± 143	4053 ± 143
Grating radius, R_g (mm)	10777	10777	14856
Grating coating	Ir	Ir	Au
Plane mirror	Mg1	Mg1	Mg2
Plane-mirror coating	Ir	Ir	Au

3. Optical layout of the beamline

3.1. Prefocusing mirror system

The Kirkpatrick–Baez focusing mirror system is used for this purpose. The first mirror, Mh, which is cylindrical, deflects and focuses the source horizontally to a position 4000 mm upstream of the refocusing mirror. Its demagnification factor is 0.7. The mirror is made of OFHC copper and its mounting is water-cooled. One half of the mirror in the beam direction is coated with nickel for the energy range 7.7–45 eV and the other half is coated with gold for 36–124 eV.

The second mirror, Mv, which is spherical, deflects and focuses the source vertically on the entrance slit of the monochromator. The 8:1 demagnification ratio was chosen to reduce the quite large source size of 640 μm ($4\Sigma_y$) to about 80 μm for obtaining high flux. It will be shown later that this demagnification ratio is acceptable for the monochromator. The aberration is 63 μm , calculated from the data given in Fig. 1 and the

effective angular divergence of 0.75 mrad ($4\Sigma'_y$) at 15 eV. The aberration from a slope error of 0.5 arcsec is 11 μm . These are reasonable compared with the entrance slit width.

3.2. Monochromator

The monochromator design is based on the Dragon spherical-grating monochromator (Chen, 1987) with the modification of inserting two plane mirrors between the entrance slit and grating as Peatman *et al.* (1989) did for the BESSY TGM-5 beamline. Thus the monochromator has two including angles of 148 and 157°, so as to cover the wide energy range with high grating efficiency, and offers the chance to choose the plane-mirror coating material to suppress high-order radiation. The plane mirror Mg1 is combined with the 450 and 900 lines mm⁻¹ line-density gratings to cover the energy range from 7.7 to 45 eV. Mg2 is combined with the 1240 lines mm⁻¹ grating to cover the energy range from 36 to 124 eV. Table 1 lists the basic parameters of the modified spherical monochromator. The parameters of the gratings are determined by arranging the maximum efficiency at the centre of the design energy range for every grating using the *Grating Efficiency Computer Code* of Neviere (1991).

The resolution contributions calculated using the analytical expressions from Chen (1987) are shown in Fig. 2. $\Delta\lambda_i/\lambda$ and $\Delta\lambda_f/\lambda$ are the entrance and exit limits, respectively. The aberration contribution, $\Delta\lambda_a/\lambda$, is proportional to the second power of the acceptance angle and is calculated with the acceptance angle at the lower energy limit, so it can be further reduced by decreasing the acceptance with an aperture for the high-energy side of the first and second gratings. The contribution from the figure slope error, $\Delta\lambda_e/\lambda$, is the limiting one for the entire energy range of the gratings. This can only be improved by good quality gratings.

Although the monochromator has two including angles, it is possible to choose a reasonable exit-arm scanning range for all the gratings. This can easily be performed using the equations from Chen (1987). First, r_1 , $r_{2,\text{min}}$ and R_g are calculated for the 157° including angle grating, and then they are calculated for the 148° including angle gratings so that r_1 is 2004 mm and $r_{2,\text{min}}$ is the same as the former. Finally, the exit-arm scanning range is calculated by solving the grating equation and meridional focusing equation with the desired energy range. The results are also shown in Fig. 2.

According to the chosen demagnification ratio of the vertical focusing mirror, the entrance-arm length, r_1 , and the maximum incidence angle of the grating, the grating length is calculated to be about 110 mm. This value is acceptable.

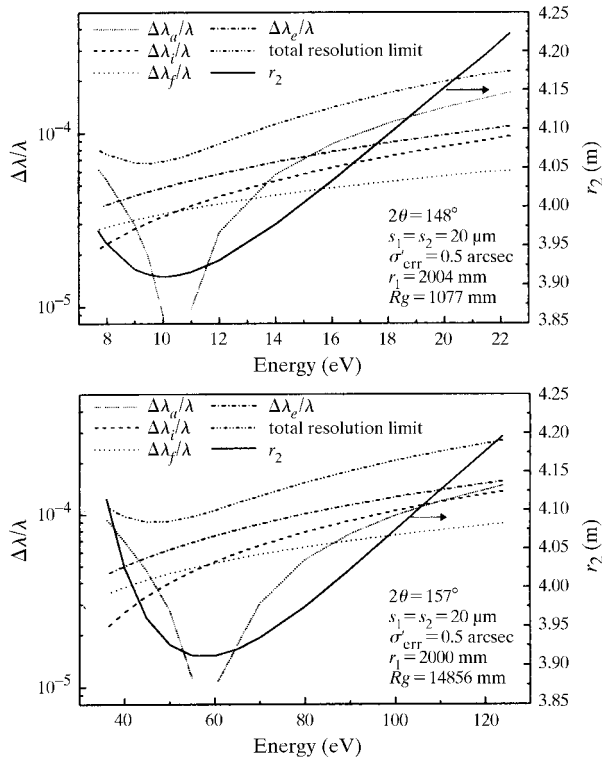


Figure 2
Various resolution limits and exit-slit position as a function of photon energy.

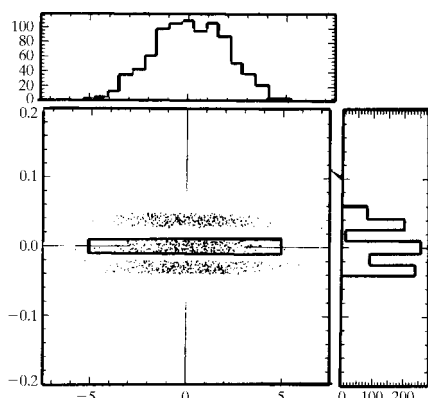


Figure 3

The image pattern and histogram distribution at the exit-slit plane for photon energies 10.0005, 10 and 9.99933 eV.

3.3. Refocusing mirror

The refocusing mirror is necessary because the experiments need a spot of about 1 mm. A toroidal mirror is used for the refocusing mirror, which focuses vertically the monochromated beam from the exit slit and focuses horizontally the image of the first mirror, Mh, to the sample position. Because the refocusing mirror generally operates under a defocusing condition in the vertical direction due to the translation of the exit slit, the spot size in the vertical direction is decided by the defocusing degree. Its maximum value is about 0.5 mm, which is acceptable. The spot size in the horizontal direction, which receives little change due to the exchange of gratings, is estimated to be about 1.5 mm from the demagnification factor of the first horizontal-focusing mirror, 0.7, and that of the refocusing mirror, 0.5. The exit-arm length of the mirror is 2000 mm, which is long enough to install a differential pumping system between the mirror and experimental chamber.

4. Performance estimation of the SGM beamline

The performance of the SGM beamline was estimated using the *SHADOW* ray-tracing package. The results confirm that the above calculation is reasonable. The image patterns at the entrance and exit slits are all straight. The spot size at the sample is about 1.5 mm (H) \times 0.5 mm (V), which was expected. The resolving power of the monochromator was checked at a few energies for every grating. At the coma-free point it is larger than 20000 for the first and second gratings and 15000 for the third grating, and at the high-energy limit it is 8000 for the former and 5000 for the latter, all with 20 μ m slit openings and without figure slope error effects. Fig. 3 shows the image pattern and histogram distribution at the exit-slit plane with 20 μ m entrance slit opening for photon energies 10.0005, 10 and 9.99933 eV, as an example.

The transmission of the beamline is calculated by the product of reflectivity of the mirrors, diffraction efficiency of the gratings and the fraction of the rays that pass through the entrance and exit slits for 0.02% bandwidth. The photon flux at the sample is obtained by the product of the transmission and the source intensity and is shown in Fig. 4.

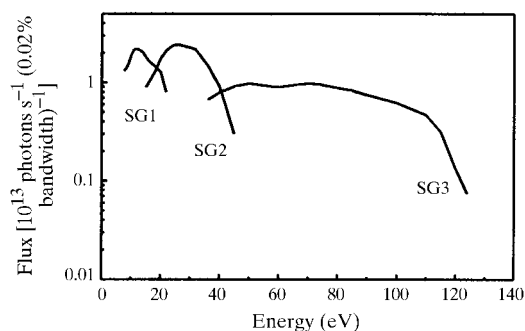


Figure 4

Photon flux at the sample for a 0.02% bandwidth.

5. Summary

The optical design of the NSRL undulator beamline is presented. The Dragon spherical-grating monochromator is used for the beamline with the modification of inserting two plane mirrors into the entrance arm of the monochromator. Calculations show that the monochromator can work for the energy range 7.7–124 eV with high grating diffraction efficiency, as expected. The resolving power at the coma-free point is larger than 20000 for the first and second gratings and 15000 for the third grating, and at the high-energy limit it is 8000 for the former and 5000 for the latter, all with 20 μ m slit openings. A flux of 10^{12} photons s^{-1} can be expected at 10 eV with an 80 μ m slit opening and 300 mA ring current.

The authors would like to acknowledge H. A. Padmore for his helpful suggestions. They are also grateful to Qika Jia, Yunlian Yan, Shaojian Xia and Qiuping Wang for useful discussions.

References

- Chen, C. T. (1987). *Nucl. Instrum. Methods*, **A256**, 595–604.
- Chen, C. T. & Sette, F. (1989). *Rev. Sci. Instrum.* **60**, 1616–1621.
- Heimann, P., Warwick, T., Howells, M., McKinney, W., Digennaro, D., Gee, B., Yee, D. & Kincaid, B. (1992). *Nucl. Instrum. Methods*, **A319**, 106–109.
- McKinney W. R., Howells, M. R., Lauritzen, T., Chin, J., Digennaro, R., Fong, E., Gath, W., Guigli, J., Hogrefe, H., Meneghetti, J. & Plate, D. (1990). *Nucl. Instrum. Methods*, **A291**, 221–224.
- Mythen, C. S., van der Laan, G. & Padmore, H. A. (1992). *Rev. Sci. Instrum.* **63**, 1313–1316.
- Neviere, M. (1991). *Grating Efficiency Computer Code*. Laboratoire d'Optique Electromagnetique, Marseille, France.
- Peatman, W., Carbone, C., Gudat, W. & Heinen, W. (1989). *Rev. Sci. Instrum.* **60**, 1445–1450.
- Peatman, W. B., Bahrtdt, J., Eggenstein, F., Reichardt, G. & Senf, F. (1995). *Rev. Sci. Instrum.* **66**, 2801–2806.
- Randall, K. J., Feldhaus, J., Erlebach, W., Bradshaw, A. M., Eberhardt, W., Xu, Z., Ma, Y. & Johnson, P. D. (1992). *Rev. Sci. Instrum.* **63**, 1367–1370.
- Shu, D., Xu, P. S., Cai, Y., Wang, W., Wang, M. T., Liu, J., Zhang, Y. J., He, W., Zheng, H. W., Zong, C. C. & Xie, Q. (1989). *Proceedings of the International Conference on Synchrotron Radiation Applications*, Hefei, pp. 346–349. Hefei: University of Science and Technology of China.